

Adaptive virtual inertia controller based on machine learning for superconducting magnetic energy storage for dynamic response enhanced

Herlambang Setiadi¹, Muhammad Abdillah², Yusrizal Afif¹, Rezi Delfianti¹

¹Faculty of Advanced Technology and Multidiscipline, Universitas Airlangga, Surabaya, Indonesia

²Department of Electrical Engineering, Universitas Pertamina, Jakarta, Indonesia

Article Info

Article history:

Received Jul 26, 2022

Revised Dec 4, 2022

Accepted Dec 7, 2022

Keywords:

Clean energy technology

Energy storage

Machine learning

Superconducting magnetic

energy storage

Virtual inertia controller

ABSTRACT

The goal of this paper was to create an adaptive virtual inertia controller (VIC) for superconducting magnetic energy storage (SMES). An adaptive virtual inertia controller is designed using an extreme learning machine (ELM). The test system is a 25-bus interconnected Java Indonesian power grid. Time domain simulation is used to evaluate the effectiveness of the proposed controller method. To simulate the case study, the MATLAB/Simulink environment is used. According to the simulation results, an extreme learning machine can be used to make the virtual inertia controller adaptable to system variation. It has also been discovered that designing virtual inertia based on an extreme learning machine not only makes the VIC adaptive to any change in the system but also provides better dynamics performance when compared to other scenarios (the overshoot value of adaptive VIC is less than -5×10^{-5}).

This is an open access article under the [CC BY-SA](https://creativecommons.org/licenses/by-sa/4.0/) license.



Corresponding Author:

Herlambang Setiadi

Faculty of Advanced Technology and Multidiscipline, Universitas Airlangga

Mulyorejo, Surabaya, Indonesia

Email: h.setiadi@ftmm.unair.ac.id

1. INTRODUCTION

Over the last few years, there has been a significant increase in the development of energy storage. This occurred as a result of the advancement of power electronics devices [1], [2]. Energy storage has the ability to store and release electricity over a short period of time. Furthermore, because energy storage can handle the uncertain power output of wind and photovoltaic, it could aid in increasing the high penetration of renewable-based power plants such as wind and photovoltaic [3]. Several energy storage systems have been used in industrial sectors and in university research. Capacitor energy storage, battery energy storage, redox flow batteries, and superconducting magnetic energy storage are all types of energy storage (SMES).

Dhundhara and Verma [4] described the use of capacitor energy storage (CES) for frequency regulation. The test system is a multisource deregulated power system that is used to investigate the impact of adding CES on frequency stability. The simulation results show that CES can regulate frequency in a multisource power system. Zhang *et al.* [5] proposed battery energy storage systems for voltage regulation. The test system is a research-active distribution system. Distributed generation is also thought to complement battery energy storage systems. It has been discovered that by co-planning distributed generation and battery energy storage systems, static voltage stability in distribution systems can be significantly improved.

Oshnoei *et al.* [6] proposed the use of a redox flow battery for a load frequency control scheme. To simulate the proposed method, two-area power systems are used as the plant. Wind turbine power plants are used to simulate inverter-based power plants. According to the simulation results, adding the redox flow battery to the system results in less overshoot and a faster settling time for the area control error. Furthermore, the

system's frequency has a lower rate of frequency change (RoCof) when compared to a system without a redox flow battery. Furthermore, when a redox flow battery is installed on the systems, the difference between mechanical and electrical power is reduced. Among these, superconducting magnetic energy storage has gained favor due to its quick response and ability to solve power system problems [7], [8]. Although SMES can be used to solve a variety of problems in power systems, when a low inertia problem arises in a power system, SMES becomes obsolete. As a result, it is critical to have an additional controller SMES so that SMES can also be used to regulate the system's total inertia. A virtual inertia controller is a name given to the controller.

Kerdphol *et al.* [9] described the use of a virtual inertia controller to improve frequency stability. The microgrid serves as the system for testing the performance of a virtual inertia controller for improving frequency stability. According to reports, adding a virtual inertia controller to the system could help it reduce the rate of frequency change. Kerdphol *et al.* [10] described the use of a virtual inertia controller for inertia emulation in a low inertia system. The microgrid is used as the test system, as in previous research, to investigate how virtual inertia control can simulate inertia in the system. The simulation shows that when energy storage is installed with proper design parameters, virtual inertia controller parameters can provide inertia emulation without the addition of a rotating machine. It is clear from the research that designing and tuning virtual inertia controller parameters is critical. Metaheuristic algorithms are commonly used to optimize the design of the virtual inertia controller.

Abo-Elyousr [11] describes the use of artificial bee colonies in the design of virtual inertia controllers. The test system is a large-scale interconnected power system. The artificial bee colony's efficacy is investigated using time domain simulation. According to the simulation results, designing the virtual inertia control using an artificial bee colony improves the system's response frequency over using a conventional virtual inertia controller alone. Saleh *et al.* [12] used manta ray foraging optimization to design a virtual inertia controller, similar to [11]. The test system is an islanded microgrid. Renewable energy sources are installed in the system to simulate low inertia conditions. The simulation results show that manta ray foraging optimization can be used to optimally design a virtual inertia controller. In [13], [14], the use of particle swarm optimization (PSO) and the firefly algorithm (FA) to optimize parameters was described. It is clear that PSO and FA can provide better parameters than traditional optimization methods. The issue arose when the system's operating conditions varied. The parameter will be optimized by the algorithm in every operating condition. In addition, each iteration algorithm necessitates a longer execution time. As a result, it is critical to create a virtual inertia controller that is adaptable to changing operating conditions. This paper proposed a novel method for designing an adaptive virtual inertia controller for superconducting magnetic energy storage based on an extreme learning machine.

2. METHOD

2.1. Inertia representation

To control the system frequency in a synchronous generator, the active power and the resulting kinetic energy function must be controlled. The rotor's rotating mass generates inertia power measured in joules-seconds ($J \cdot s$) or watt-seconds squared ($W \cdot s^2$). This inertia power is used to compensate for a disturbance during the first 1 to 5 seconds of operation or when the primary and secondary controls are not activated. Based on the swing equation, the inertial response of a synchronous machine can be written as follows, as described in (1) [15],

$$J_S \frac{d\omega}{dt} = T_m - T_e = \frac{P_m}{\omega} - \frac{P_e}{\omega} \quad (1)$$

where J_S , ω , T_m , T_e , P_m , P_e , is the moment of inertia, rotor speed, mechanical torque, electrical torque, mechanic power, and electrical power. The (2) and (3) describe the mathematical representation of inertia (3). Where S is the synchronous generator's power rating output [16].

$$H = \frac{E_{kinetik}}{S} \quad (2)$$

$$E_{kinetik} = \frac{1}{2} J_S \omega^2 \quad (3)$$

when the system is made up of several interconnected generators, the total inertia constant is the ratio of the kinetic energy of each generator added together. Furthermore, the system output power rating influences the inertia constant. As a result, referring to the total inertia can be written using (4) [17],

$$H = \frac{\sum_i (H_i S_{SGi})}{S_{PS}} \quad (4)$$

where the system's minimum inertia can be used to solve two major dynamic problems. The first issue is lowering the rate of change of frequency (*RoCof*) after the perturbation appears. The second issue is to dampen frequency overshoot and limit frequency nadir when there is a disturbance in the system. *RoCof* is the deferential frequency used to calculate the system's inertia response. The system's *RoCof* value should be limited to ± 1 Hz/s. *RoCof*'s mathematical representation can be described using (5) [18]. Where f_0 is the nominal frequency of the system.

$$RoCof = \frac{d(\Delta f)}{dt} = \frac{f_0(P_m - P_e)}{2HS} \quad (5)$$

2.2. Dynamic representation of virtual inertia controller

The virtual inertia controller (VIC) operates on the implementation of the swing equation applied to the inverter-based power plant so that the inverter, which lacks inertia, can be controlled to mimic the inertia characteristics possessed by generators in general. The term "virtual inertia" refers to the ability of the generator's rotor characteristics to be emulated without the use of any rotating mass. Controllers to emulate virtual rotors are used to control how much additional inertia power output is required by the system. The virtual inertia itself is represented as a proportional and derivative controller. Furthermore, the proportional controller is represented as virtual damping while the derivative controller is represented as virtual inertia. The dynamic equation for imitating a virtual rotor is written as (6) [19].

$$\Delta VIC = \frac{K_j s + K_d}{1} (\Delta f) \quad (6)$$

The value of virtual inertia is determined based on a derivative technique that determines the magnitude of the change in frequency (df/dt) or the rate of change of frequency (*RoCoF*) so that the amount of active power compensation in the system can be adjusted. Virtual inertia itself is used to reduce frequency overshoot. Virtual damping is used to quickly restore system frequency stability after contingency and penetration of new renewable energy generators in the electric power system. This virtual damping can mimic the effect of the damper winding on a synchronous generator [20].

2.3. SMES dynamic

SMES is used in an electric power system to control the power balance in the synchronous generator during dynamic periods [21]. On the power system model, SMES are installed in terminal bus generators [22]. A Y-transformer, a voltage source converter based on a GTO thyristor, a two-quadrant DC-DC chopper based on a GTO, and a superconducting coil comprise the basic SMES configuration. The DC-DC converters and chopper are linked by DC link capacitors [23]. The dynamic characteristics of SMES are critical in this paper. The dynamic characteristic of SMES can be captured through Laplace representation as described in (7) and (8), where k_d is the gain for feedback I_d , T_{dc} is the converter time delay, k_0 is the gain constant, and L is the coil inductance [24]. The deviation in the SMES unit's inductor real power is expressed in the time domain as described in (9). In addition, the energy stored in SMES can be mathematically described in (10) [25].

$$\Delta E_d = \frac{1}{1 + T_{dc}s} [k_0 \Delta VIC - k_d \Delta I_d] \quad (7)$$

$$\Delta I_d = \frac{1}{Ls} \Delta E_d \quad (8)$$

$$\Delta P_{smes}(t) = \Delta I_{d0} \Delta E_d + \Delta I_d \Delta E_d \quad (9)$$

$$W_{smes}(t) = \frac{LI_d^2}{2} \quad (10)$$

2.4. Extreme learning machine

Setiadi *et al.* [26] explained that the artificial neural network-based extreme learning machine (ELM) is a new learning method invented by Huang. It is a feedforward neural network with a single hidden layer, also known as a single hidden layer feedforward neural network. ELM's learning method was created to address the drawbacks of the feedforward neural network method. The disadvantage of feedforward neural networks is their learning execution time. There are two reasons why feedforward neural networks have a slow learning rate [27]: for training, slow gradient-based learning algorithms are used. The iteration from the training process defines the parameter in the network.

In the learning process, traditional gradient-based learning algorithms methods such as backpropagation (BP) or Lavenberg–Marquardt (LM) and others with manually determined feedforward neural

network (FNN) parameters are used. These parameters are input weight and hidden bias, and they are also linked from one layer to the next. As a result, it necessitates a slow learning rate and is frequently stuck at the local minimum. The input weight and hidden bias in the ELM method can be chosen at random, allowing ELM to learn quickly and produce good generalizations. The structure of the ELM method is depicted in Figure 1.

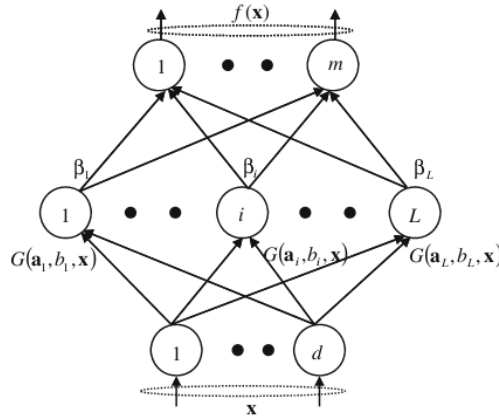


Figure 1. ELM structure

For example, if N different samples are $(x_i, t_i) \in R^d \times R^m$, the mathematical representation of standard single-hidden layer feedforward neural networks (SLFNs) with L hidden node is described in (11) [28].

$$\sum_{i=1}^L \beta_i g_i(x_j) = \sum_{i=1}^L \beta_i G(a_i, b_i, x_j) = o_j, j = 1, \dots, N \tag{11}$$

SLFNs could predict this N sample with the mean error using (12). This can happen because there are a_i, b_i and β_i . Hence the equation can be described using (13).

$$\sum_{i=1}^L \|o_j - t_j\| = 0 \tag{12}$$

$$\sum_{i=1}^L \beta_i G(a_i, b_i, x_j) = o_j, j = 1, \dots, N \tag{13}$$

We can further simplify (13) as described in (14) to (17). H is the matrix output hidden layer from SLFNs, column i^{th} from H is the output from hidden node i^{th} that connected with the input $x_1, x_2, x_3, \dots, x_N$. In addition, feature mapping of hidden layers is described as $h(x) = G(a_1, b_1, x_N), \dots, G(a_L, b_L, x_N)$. Row i^{th} in matrix H is a mapping feature of the hidden layer that is related to the i^{th} input from $x_i: h(x_i)$. β is the matrix from weight output and T is the target matrix or the output of ELM [29].

$$H \times \beta = T \tag{14}$$

$$H = \begin{bmatrix} h(x_1) \\ \vdots \\ h(x_N) \end{bmatrix} \tag{15}$$

$$H = \begin{bmatrix} G(a_1, b_1, x_1) & \dots & G(a_L, b_L, x_1) \\ \vdots & \dots & \vdots \\ G(a_1, b_1, x_N) & \dots & G(a_L, b_L, x_N) \end{bmatrix} \tag{16}$$

$$\beta = \begin{bmatrix} \beta_1^T \\ \vdots \\ \beta_L^T \end{bmatrix} \text{ and } T = \begin{bmatrix} T_1^T \\ \vdots \\ T_L^T \end{bmatrix} \tag{17}$$

In ELM, weight input and hidden bias are defined randomly. Hence, weight output that has a relation with the hidden layer can be described using (18) [30].

$$\beta = H^T \times T \tag{18}$$

2.5. Implementation

The section depicts the method’s implementation process (adaptive VIC on SMES based on ELM). The goal of this process is to make the VIC more adaptable to the uncertainty of system operating conditions. This training uses real power (P) and reactive power as input data (Q), while the output (predicted) parameter is the VIC parameter, K_j and K_d .

The adaptive VISMA procedure consists of the following steps.

- 1) Provide the training data of actual VIC condition.
- 2) Conduct the training process
- 3) Calculate the precision of the predicted parameter using mean absolute error (19),

$$MSE = \sum_{i=1}^N \frac{(\hat{y}_i - y_i)^2}{N} \tag{19}$$

where \hat{y}_i is the predicted data produced by the proposed learning algorithm, and y_i is the actual data. N denotes the number of data points used in the training phase.

- 4) Print the results if the MSE value is the smallest. If not, proceed to step 3 until the minimum MSE is obtained.

3. RESULTS AND DISCUSSION

This section concentrated on the experimental results and paper discussion. The test system is the 25-bus Java Indonesian power grid, which is used to demonstrate the efficacy of the proposed controller method. The Suralaya bus now includes SMES. The Suralaya bus is bus number one (represented as G1 in Figure 2). Suralaya has the highest generation capacity (3,059 MW) on the west side of Java. The generator serves as the system’s reference point. As a result, it is critical to maintain stable conditions by incorporating SMES to smooth the frequency response of the Suralaya power plant (detailed data on the Java Indonesian power grid is attached as an appendix of the paper). The system is implemented in the MATLAB/Simulink environment. Figure 3 depicts a single-line diagram of the Java Indonesia power grid.

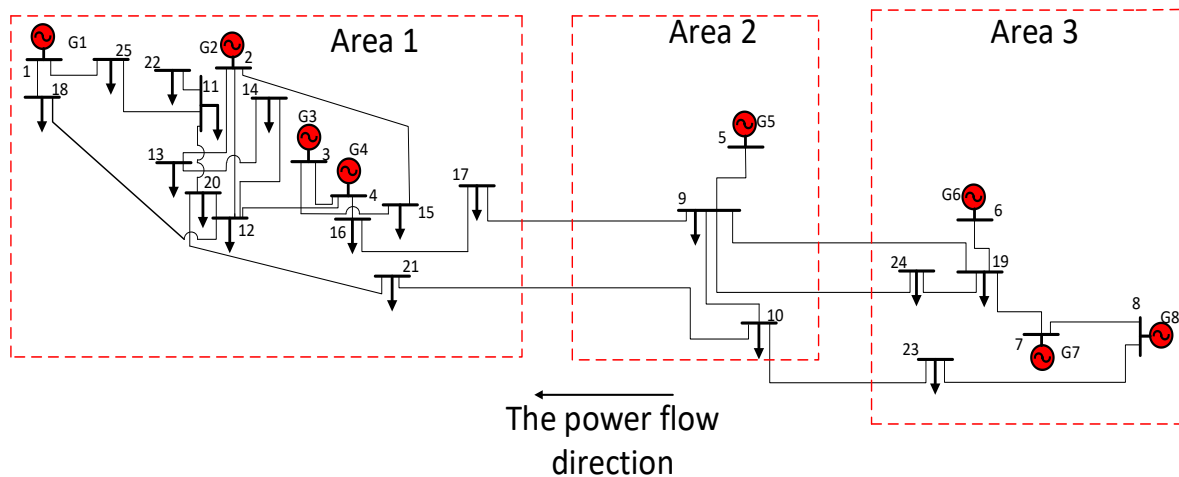


Figure 2. Single line diagram of Java-Bali Indonesian power grid

This section examines the performance of the proposed method using three different case studies. The first case study demonstrates the capabilities of ELM in training VIC data (training phased). The performance of VIC training data in non-linear time domain simulation is demonstrated in the second case study (testing phased). In addition, in the second case study, a comparison of VIC-based ELM and conventional VIC is performed. The final case study is a comparison phased case study. In this case study, comparisons between different algorithm methods and the proposed method are made to demonstrate the efficacy of the paper’s proposed method.

3.1. Training phase

In this step, an investigation of the ELM performance for training the VIC-optimized parameter is conducted, where the input of ELM is the active and reactive power variation. In addition, the output of ELM is the VIC parameter. Figure 3 depicts a comparison of K_j conventional and K_j based on ELM. Figure 4 shows a comparison of K_d conventional and K_d -based ELM. It is clear that ELM can replicate the value of VIC conventional.

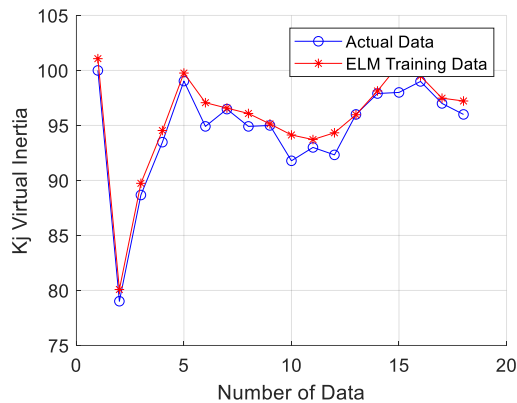


Figure 3. K_j trained parameter

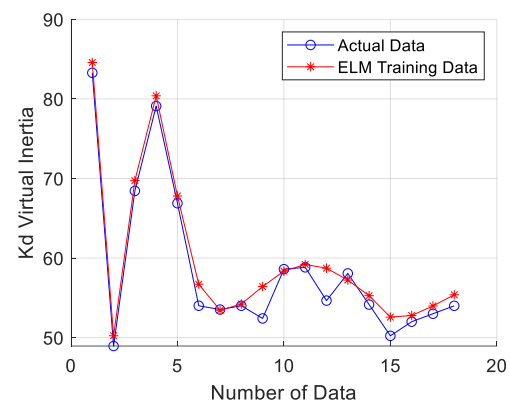


Figure 4. K_d trained parameter

ELM takes only 0.0625 seconds to execute in order to find the trained parameter. Furthermore, Figure 3 shows that the maximum error for K_j is 2.5548 and the minimum error is 0.0285. The maximum error for K_d value is 4.0757, while the minimum error for K_d value is 0.2471, as shown in Figure 4. Based on these findings, it is possible to conclude that the ELM can estimate the VIC value based on the operating conditions.

3.2. Testing phase

The trained VIC will be tested against a disturbance in this case study. This study considers 0.05 load change to investigate how the system performs in the face of disturbance. To investigate the efficacy of the proposed method, two different scenarios are considered. The system with VIC actual data is the first scenario. The second scenario is an ELM-based system with VIC (proposed method). The dynamic response of the frequency in area 1 is depicted in Figure 5. With VIC actual data, the blue line represents the dynamic frequency response in area 1. The red line represents the dynamic frequency response with VIC based on ELM in area 1.

From Figure 5, it is observed that the response between the system with VIC actual data and VIC-ELM is almost similar. Hence, it can be concluded that the ELM can mimic the performance of VIC actual data. In addition, from Figure 5, it is noticeable that the response of the system with VIC-ELM is better than the system with VIC actual data. It is found that a system with VIC-ELM can give less overshoot compared to the VIC actual data. Furthermore, to further investigate the efficacy of VIC-based ELM comparison with different technique need to be conducted.

3.3. Comparison phase

In this section, the comparison of the proposed method with the existing method is carried out. The simulation has been done by giving 0.05 load changing in area 1. Figure 6 shows the time domain response of the frequency dynamic response of the Suralaya power plant. Different artificial intelligence (AI) is considered in this section. The first AI is PSO. The second AI is the FA, while the last AI is our proposed method. The VIC-SMES based on PSO is indicated by the blue line while the VIC-SMES-based FA is represented with the red line. In addition, the purple line indicates our proposed method. From the simulation results, it is observed that the best performance is given by ELM. This is indicated by the smallest overshoot and fastest settling time compared to the PSO and FA methods. This could be happening because the VIC-SMES-based ELM could give a more detailed control signal. Hence, the SMES could provide detailed active power that can act as virtual inertial control to the systems.

For further information regarding the efficacy of the proposed method, an execution time comparison between the proposed method with PSO and FA is carried out. Table 1 shows the execution time of each method for finding the optimal value of VIC-SMES. The proposed method shows the fastest execution time compared to PSO and FA. As the PSO and FA is optimization method, they need more time to find their optimal

value. It is also depending on how much the complexity of the system. Different from ELM, ELM is a training method. They do not need a lot of time to train the data. The proposed method could find an optimal value of less than a second while PSO and FA need more than 3 minutes to find the optimal solution of VIC-SMES.

Three different transient indices are used to investigate the efficacy of the VIC-based ELM in comparison to the VIC-based PSO and FA. Integral time absolute error (ITAE), integral absolute error (IAE), and integral square error are the three indices (ISE). Table 2 compares the indices of VIC-based ELM, VIC-based PSO, and VIC-based FA. For all three indices, it is discovered that the VIC-based ELM outperforms the VIC-based FA and VIC-based PSO.

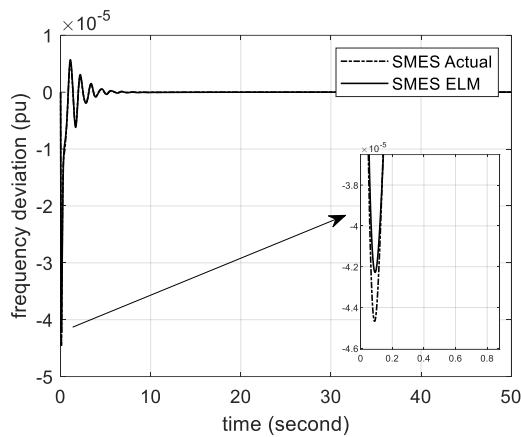


Figure 5. Frequency response comparison

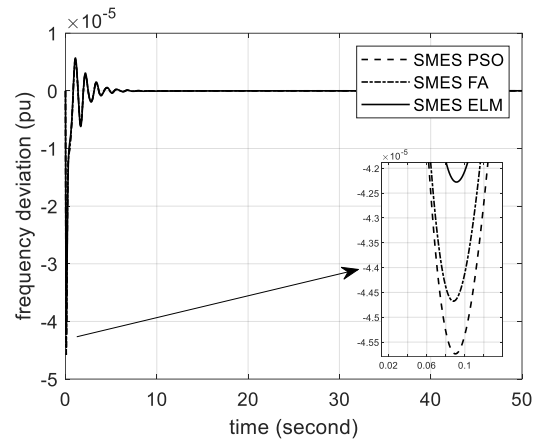


Figure 6. Frequency dynamics response comparison

Table 1. Detailed execution time

Index	PSO	FA	ELM
Execution time	10 minutes	5 minutes	0.03 second

Table 2. Transient response indices comparison

Index	PSO	FA	ELM
ITAE	3.227×10^{-5}	3.339×10^{-5}	3.358×10^{-5}
IAE	1.71×10^{-5}	1.95×10^{-5}	2.01×10^{-5}
ISE	3.239×10^{-10}	3.249×10^{-10}	3.25×10^{-10}

4. CONCLUSION

This paper proposed a novel method of adaptive virtual inertia controller based on an extreme learning machine for superconducting magnetic energy storage. The goal of this paper is to improve the dynamic performance of power systems using SMES and adaptive VIC. The power grid of Java, Indonesia, is used as a test system to demonstrate the efficacy of the proposed controller method. According to simulation results, extreme learning machines can train VIC to be adaptive to any operating condition variation. It has also been discovered that VIC ELM can mimic the performance of conventional VIC while producing better results. Furthermore, it is discovered that the proposed control method outperforms the other methods presented in this paper. Implementing a more advanced type of machine learning for VIC parameter training can be used to conduct additional research. In addition, considering the inverter-based power plant integration could also be a further study to make the system more up-to-date and realistic.

ACKNOWLEDMENT

The corresponding author wishes to express gratitude to Universitas Airlangga for funding this study by the “*Penelitian Dosen Pemula*” grant (No. 416/UN3.1.17/PT/2023).

REFERENCES

- [1] H. Setiadi *et al.*, “Multi-mode damping control approach for the optimal resilience of renewable-rich power systems,” *Energies*, vol. 15, no. 9, Apr. 2022, doi: 10.3390/en15092972.

- [2] M. Meliani, A. El Barkany, I. El Abbassi, A. M. Darcherif, and M. Mahmoudi, "Energy management in the smart grid: State-of-the-art and future trends," *International Journal of Engineering Business Management*, vol. 13, Jan. 2021, doi: 10.1177/18479790211032920.
- [3] M. Meliani, A. El Barkany, I. El Abbassi, R. Absi, and M. Mahmoudi, "Energy management of a fuzzy control system in a microgrid," *E3S Web of Conferences*, vol. 353, Jun. 2022, doi: 10.1051/e3sconf/202235302002.
- [4] S. Dhundhara and Y. P. Verma, "Capacitive energy storage with optimized controller for frequency regulation in realistic multisource deregulated power system," *Energy*, vol. 147, pp. 1108–1128, Mar. 2018, doi: 10.1016/j.energy.2018.01.076.
- [5] Y. Zhang, Y. Xu, H. Yang, and Z. Y. Dong, "Voltage regulation-oriented co-planning of distributed generation and battery storage in active distribution networks," *International Journal of Electrical Power & Energy Systems*, vol. 105, pp. 79–88, Feb. 2019, doi: 10.1016/j.ijepes.2018.07.036.
- [6] S. Oshnoei, A. Oshnoei, A. Mosallanejad, and F. Haghjoo, "Novel load frequency control scheme for an interconnected two-area power system including wind turbine generation and redox flow battery," *International Journal of Electrical Power & Energy Systems*, vol. 130, Sep. 2021, doi: 10.1016/j.ijepes.2021.107033.
- [7] M. G. Molina and P. E. Mercado, "Power flow stabilization and control of microgrid with wind generation by superconducting magnetic energy storage," *IEEE Transactions on Power Electronics*, vol. 26, no. 3, pp. 910–922, Mar. 2011, doi: 10.1109/TPEL.2010.2097609.
- [8] A. Pappachen and A. P. Fathima, "Load frequency control in deregulated power system integrated with SMES–TCPS combination using ANFIS controller," *International Journal of Electrical Power & Energy Systems*, vol. 82, pp. 519–534, Nov. 2016, doi: 10.1016/j.ijepes.2016.04.032.
- [9] T. Kerdphol, F. S. Rahman, M. Watanabe, and Y. Mitani, "Robust virtual inertia control of a low inertia microgrid considering frequency measurement effects," *IEEE Access*, vol. 7, pp. 57550–57560, 2019, doi: 10.1109/ACCESS.2019.2913042.
- [10] T. Kerdphol, F. S. Rahman, Y. Mitani, M. Watanabe, and S. Kufeoglu, "Robust virtual inertia control of an islanded microgrid considering high penetration of renewable energy," *IEEE Access*, vol. 6, pp. 625–636, 2018, doi: 10.1109/ACCESS.2017.2773486.
- [11] F. K. Abo-Elyousr, "Load frequency controller with virtual inertia generator for Interconnected power systems via artificial bee colony," in *2018 Twentieth International Middle East Power Systems Conference (MEPCON)*, Dec. 2018, pp. 367–372, doi: 10.1109/MEPCON.2018.8635143.
- [12] A. Saleh, W. A. Omran, H. M. Hasanien, M. Tostado-Véliz, A. Alkukahyil, and F. Jurado, "Manta ray foraging optimization for the virtual inertia control of islanded microgrids including renewable energy sources," *Sustainability*, vol. 14, no. 7, Apr. 2022, doi: 10.3390/su14074189.
- [13] H. K. Abdulkhader, J. Jacob, and A. T. Mathew, "Fractional-order lead-lag compensator-based multi-band power system stabiliser design using a hybrid dynamic GA-PSO algorithm," *IET Generation, Transmission & Distribution*, vol. 12, no. 13, pp. 3248–3260, Jul. 2018, doi: 10.1049/iet-gtd.2017.1087.
- [14] M. Singh, R. N. Patel, and D. D. Neema, "Robust tuning of excitation controller for stability enhancement using multi-objective metaheuristic Firefly algorithm," *Swarm and Evolutionary Computation*, vol. 44, pp. 136–147, Feb. 2019, doi: 10.1016/j.swevo.2018.01.010.
- [15] T. Kerdphol, F. S. Rahman, M. Watanabe, and Y. Mitani, *Virtual inertia synthesis and control*. Cham: Springer International Publishing, 2021, doi: 10.1007/978-3-030-57961-6.
- [16] P. S. Kundur, *Power system stability and control*. McGraw Hill, 1994.
- [17] H. Bevrani, B. Francois, and T. Ise, *Microgrid dynamics and control*. Hoboken, NJ, USA: John Wiley & Sons, Inc., 2017, doi: 10.1002/9781119263739.
- [18] H. Bevrani, *Robust power system frequency control*. Boston, MA: Springer US, 2009, doi: 10.1007/978-0-387-84878-5.
- [19] T. Kerdphol, M. Watanabe, K. Hongesombut, and Y. Mitani, "Self-adaptive virtual inertia control-based fuzzy logic to improve frequency stability of microgrid with high renewable penetration," *IEEE Access*, vol. 7, pp. 76071–76083, 2019, doi: 10.1109/ACCESS.2019.2920886.
- [20] S. K. Singh, R. Singh, H. Ashfaq, and R. Kumar, "Virtual inertia emulation of inverter interfaced distributed generation (IIDG) for dynamic frequency stability & damping enhancement through BFOA tuned optimal controller," *Arabian Journal for Science and Engineering*, vol. 47, no. 3, pp. 3293–3310, Mar. 2022, doi: 10.1007/s13369-021-06121-5.
- [21] H. Zhang *et al.*, "Design and control of a new power conditioning system based on superconducting magnetic energy storage," *Journal of Energy Storage*, vol. 51, Jul. 2022, doi: 10.1016/j.est.2022.104359.
- [22] N. Mughees, M. H. Jaffery, and M. Jawad, "A new predictive control strategy for improving operating performance of a permanent magnet synchronous generator-based wind energy and superconducting magnetic energy storage hybrid system integrated with grid," *Journal of Energy Storage*, vol. 55, Nov. 2022, doi: 10.1016/j.est.2022.105515.
- [23] K. M. Kotb, M. F. Elmorshedy, H. S. Salama, and A. Dán, "Enriching the stability of solar/wind DC microgrids using battery and superconducting magnetic energy storage based fuzzy logic control," *Journal of Energy Storage*, vol. 45, Jan. 2022, doi: 10.1016/j.est.2021.103751.
- [24] K. Iyswarya Annapoorani, V. Rajaguru, S. Anantha Padmanabhan, K. Manoj Kumar, and S. Venkatachalam, "Fuzzy logic-based integral controller for load frequency control in an isolated micro-grid with superconducting magnetic energy storage unit," *Materials Today: Proceedings*, vol. 58, pp. 244–250, 2022, doi: 10.1016/j.matpr.2022.02.103.
- [25] C. N. S. Kalyan *et al.*, "Comparative performance assessment of different energy storage devices in combined LFC and AVR analysis of multi-area power system," *Energies*, vol. 15, no. 2, Jan. 2022, doi: 10.3390/en15020629.
- [26] H. Setiadi *et al.*, "An extreme learning machine based adaptive VISMA for stability enhancement of renewable rich power systems," *Electronics*, vol. 11, no. 2, Jan. 2022, doi: 10.3390/electronics11020247.
- [27] I. Manuaba, M. Abdillah, R. Zamora, and H. Setiadi, "Adaptive power system stabilizer using kernel extreme learning machine," *International Journal of Intelligent Engineering and Systems*, vol. 14, no. 3, pp. 468–480, Jun. 2021, doi: 10.22266/ijies.2021.0630.39.
- [28] B. Liu, G. Chen, H.-C. Lin, W. Zhang, and J. Liu, "Prediction of IGBT junction temperature using improved cuckoo search-based extreme learning machine," *Microelectronics Reliability*, vol. 124, Sep. 2021, doi: 10.1016/j.microrel.2021.114267.
- [29] P. Pi and D. Lima, "Gray level co-occurrence matrix and extreme learning machine for Covid-19 diagnosis," *International Journal of Cognitive Computing in Engineering*, vol. 2, pp. 93–103, Jun. 2021, doi: 10.1016/j.ijcce.2021.05.001.
- [30] A. Yousaf, R. M. Asif, M. Shakir, A. U. Rehman, and M. S. Adrees, "An improved residential electricity load forecasting using a machine-learning-based feature selection approach and a proposed integration strategy," *Sustainability*, vol. 13, no. 11, May 2021, doi: 10.3390/su13116199.

BIOGRAPHIES OF AUTHORS

Herlambang Setiadi    is a lecturer at Faculty Advanced Technology and Multidiscipline Universitas Airlangga. He received a bachelor's degree from Institut Teknologi Sepuluh Nopember (Surabaya, Indonesia) majoring in power system engineering in 2014, then a master's degree from Liverpool John Moores University, Liverpool, United Kingdom, majoring in electrical power and control engineering in 2015. Furthermore, he received a doctoral degree from The University of Queensland. His research interests are power system dynamics and control, renewable energy integration, and metaheuristic algorithm. He can be contacted at h.setiadi@ftmm.unair.ac.id.



Muhammad Abdillah    was born in Pasuruan. He received *Sarjana Teknik* (equivalent to B.Eng.), and *Magister Teknik* (equivalent to M.Eng.) degrees from the Department of Electrical Engineering, Institut Teknologi Sepuluh Nopember (ITS), Surabaya, Indonesia in 2009 and 2013, respectively. He obtained a Dr. Eng. degree from the Graduate School of Engineering, Hiroshima University, Japan in 2017. He is currently working as a lecturer at the Department of Electrical Engineering, Universitas Pertamina, Jakarta, Indonesia. As author and co-author, he had published 100 scientific papers in different journals and conferences. He was a member of IEEJ, IAENG and IEEE. His research interests are power system operation and control, power system optimization, robust power system security, power system stability, intelligent control and system, and artificial intelligence (optimization, machine learning, deep learning). He can be contacted at m.abdillah@universitaspertamina.ac.id.



Yusrizal Afif    was born in Surabaya, East Java, Indonesia in 1992. He received bachelor and engineering degree in electrical engineering from Institut Teknologi Sepuluh Nopember, Surabaya, Indonesia, in 2015. From 2015 to 2017 he worked as an electrical engineer at Krakatau Engineering Co., Indonesia. He received a Master Engineering degree in electrical engineering from Institut Teknologi Sepuluh Nopember in 2019. He joined Airlangga University in 2020 as a lecturer. His research concentrates mainly on high voltage technology, apparatus characteristics, discharge phenomena, and renewable energy. He can be contacted at yusrizal@ftmm.unair.ac.id.



Rezi Delfianti    received a B.Eng degree in the Electrical Engineering Department at Yogyakarta State University and a Master of Engineering degree in the Electrical Engineering Department at Sepuluh Nopember Institute of Technology, Surabaya, Indonesia. She is now pursuing her doctorate in the Electrical Engineering Department at Sepuluh Nopember Institute of Technology, Surabaya, Indonesia. She presently works as a lecturer in electrical engineering at the Faculty of Advanced Technology and Multidiscipline at Airlangga University Surabaya, Indonesia. Her research interests include solar energy stability, economics, optimization, and artificial intelligence. She can be contacted at rezi.delfianti@ftmm.unair.ac.id.